Molecular Vision 2026; 32:435-449 <http://www.molvis.org/molvis/v32/435>
Received 16 January 2026 | Accepted 23 July 2026 | Published 25 September 2026

© 2026 Molecular Vision

PEDF regulates the photoreceptor transcription factor CRX via PEDF-R in the retina

Shivani Dixit,[1] Ivan T. Rebustini,[1] Susan E. Crawford,[2] S. Patricia Becerra[1]

[1]Section of Protein Structure and Function, Laboratory of Retinal Cell and Molecular Biology, National Eye Institute, National Institutes of Health, Bethesda, MD; [2]Department of Cancer Biology, Endeavor Health Research Institute, Affiliate of University of Chicago Pritzker School of Medicine, Evanston, IL

Purpose:: The transcription factor CRX regulates the expression of *Pde6b*, which is mutated in the *rd10* mouse model of retinitis pigmentosa, leading to progressive photoreceptor degeneration. Pigment epithelium-derived factor (PEDF) is a neurotrophic factor that promotes survival through its receptor PEDF-R in models of retinal degeneration (e.g., *rd10*), and its absence increases photoreceptor susceptibility to degeneration. This study investigates CRX expression changes regulated by PEDF in retinal degeneration models.

Methods:: Wild-type (C57B6J), PEDF-deficient (*Serpinf1*$^{-/-}$), PEDF-R–deficient (*Pnpla2*$^{-/-}$), *rd10*, and *rd10/Serpinf1*$^{-/-}$ mice were used. Retinal explants were prepared and zaprinast was used to induce photoreceptor cell death. Treatments included a PEDF[H105A] variant, PEDF-derived peptides (H105A, R99A), and atglistatin (a PEDF-R inhibitor). H105A was also administered via eye drops. *Crx* transcript levels and CRX protein were assessed using quantitative reverse transcription polymerase chain reaction and immunofluorescence, respectively.

Results:: In the absence of PEDF or PEDF-R, CRX levels in photoreceptors were diminished. PEDF[H105A] treatment restored CRX levels in retinal explants and mitigated zaprinast-induced changes in CRX nuclear distribution. H105A peptide eye drops transiently increased retinal *Crx* expression in *rd10* and *rd10/Serpinf1*$^{-/-}$ mice in vivo. In wild-type explants, PEDF[H105A] and the H105A peptide elevated CRX protein levels, whereas R99A (lacking PEDF-R affinity) had no effect. PEDF-R inhibition by atglistatin abolished H105A-mediated CRX upregulation.

Conclusion:: These findings identify CRX as a likely downstream component of PEDF-mediated signaling in photoreceptors. PEDF treatment increased CRX expression and promoted its nuclear localization in a PEDF-R–dependent manner, supporting a role for the PEDF/PEDF-R signaling pathway in regulating CRX in the retina.

Pigment epithelium-derived factor (PEDF) is a multifunctional protein that has emerged as a promising neuroprotective candidate in retinal degeneration research. Numerous studies have shown that PEDF protects retinal tissues from various insults, including serum starvation, apoptosis, oxidative stress, and inflammation, by modulating key signaling pathways involved in cell survival [1,2]. Its importance is particularly evident in mouse models, such as *rd1* and *rd10* mice, both of which carry mutations in the *phosphodiesterase 6B* (*Pde6b*) gene and serve as robust models for studying autosomal recessive retinitis pigmentosa [3–6]. We previously demonstrated that the absence of serine protease inhibitor 1 (*Serpinf1*; the gene encoding PEDF) exacerbates photoreceptor cell death and accelerates retinal degeneration in *rd10* models [7]. Conversely, PEDF administration delays photoreceptor death in the *rd10* and other inherited retinal degeneration models [2,5,8].

Correspondence to: S. Patricia Becerra, National Institutes of Health, National Eye Institute, 6 Center Dr. Bethesda, MD 20892; FAX: (301) 451-5420 Phone: (301) 496-6514; email: becerras@nei.nih.gov

The molecular mechanism underlying the protective effects of PEDF involves its receptor, PEDF-R (also known as ATGL, desnutrin, iPLA2ζ, PNPLA2, coded by *Pnpla2*, patain-like phospholipase A2), by activating its phospholipase activity to liberate fatty acids such as docosahexaenoic acid from phospholipids [9–11]. This cascade facilitates calcium ion extrusion, thereby preventing the activation of calcium-dependent proteases, such as calpain [12]. These events increase the cellular BCL2/BAX ratio and prevent apoptosis-inducing factor translocation from mitochondria to the nucleus, ultimately promoting cell survival [12]. Importantly, small peptides derived from the receptor-binding domain of PEDF, such as 17-mer and H105A, are bioactive and replicate the neurotrophic signaling cascade observed with the full-length PEDF protein [6,12,13].

Despite these advances, the downstream mechanisms linking the extracellular signaling function of PEDF to nuclear targets in degenerating photoreceptors remain poorly understood. A key regulator of photoreceptor development and maintenance is the photoreceptor-specific transcription factor cone-rod homeobox (CRX) [14], which controls a range of genes critical for photoreceptor development,

differentiation, function, and survival [15]. Mutations in *Crx* result in abnormal photoreceptor development and are associated with congenital blindness, photoreceptor dysfunction, or death [16,17]. While the role of CRX in development is well established, its involvement in photoreceptor homeostasis and survival during retinal degeneration remains largely unexplored. Because *Pde6* is a target gene of CRX, we hypothesize that PEDF signaling may engage with CRX to promote photoreceptor survival.

To investigate the impact of the neurotrophic PEDF on CRX expression and function in the retina, we used mouse retinal explants, a PDE6 inhibitor to induce photoreceptor death, and genetic variants with *Pde6* mutations. Our results show that PEDF enhances CRX expression and promotes its nuclear localization via PEDF-R, demonstrating for the first time that CRX is a key mediator of the photoreceptor survival-enhancing effects of PEDF. This study highlights the critical role of CRX in photoreceptor resilience during retinal degeneration and provides insights into how PEDF links extracellular survival signals to nuclear mechanisms. These findings offer a foundation for developing targeted therapies to preserve vision in retinal degenerative diseases.

METHODS

Animals: The mice used in this study were *C57BL/6J* and *rd10* from The Jackson Laboratory (Bar Harbor, ME), *Serpinf1*$^{-/-}$ and *Pnpla2*$^{-/-}$ as previously described [7,18,19], and *rd10/Serpinf1*$^{-/-}$, generated by crossing homozygous *rd10* mice with *Serpinf1*$^{-/-}$ mice, as previously described [7]. All mice (postnatal 15 days (P15) to 3 months of age, mixed sexes, and *rd8*-free) were maintained in the animal facility of the National Institutes of Health. All animal experimental procedures were approved by the National Eye Institute Animal Care and Use Committee and were performed as per the guidelines of the Association for Research in Vision and Ophthalmology statement for the Use of Animals in Ophthalmic and Vision Research and in accordance with the ARRIVE guidelines. All experimental animals were maintained on a normal chow diet and a 12-h light/12-h dark cycle.

Mouse genotyping was provided by a commercially available automated service from Transnetyx (Memphis, TN, USA). *Serpinf1*$^{-/-}$, *Pnpla2*$^{-/-}$, *Serpinf1*$^{+/+}$, and *Pnpla2*$^{+/+}$ mice were used at 12 weeks of age for retinal whole mounts and explants. The *rd10* and *rd10/Serpinf1*$^{-/-}$ mice were used at postnatal day 15 (P15) for PEDF-derived peptide eyedrops experiments.

Retinal explant culture: Basal chemically defined serum-free R16 medium was prepared using Advanced DMEM/F-12 (cat. #12634–10; ThermoFisher Scientific, Waltham, MA) supplemented with 5% GlutaMAX (100×; cat. #35050061; ThermoFisher Scientific), 1% penicillin–streptomycin (100×; cat. #15140122; ThermoFisher Scientific), and 2.56 mg/ml cytidine 5′-diphosphocholine sodium salt hydrate (cat. #30290; Millipore-Sigma, St. Louis, MO). Complete R16 medium was prepared by adding several supplements to the basal medium as described in previous studies [20,21]. Eyes from 12- to 14-week-old mice were enucleated, washed in phosphate-buffered saline (PBS), and placed in prewarmed basal R16 culture medium to maintain tissue viability and integrity. Using a dissection microscope, the eyes were dissected by making an incision at the corneal–scleral junction. The anterior segment, including the cornea, lens, and vitreous, was carefully removed to expose the posterior eyecup. The neural retina was then gently separated from the underlying eyecup, which consists of the retinal pigment epithelium (RPE), choroid, and sclera. Fine surgical forceps and histologic brushes were used for dissection to minimize mechanical stress and potential tissue damage. Four radial cuts were made in the neural retinas, creating a cloverleaf shape to allow them to lie flat. The retinas were then carefully transferred to 24-mm Transwell inserts with 0.4-µm pore polycarbonate membranes (cat. #3412; Corning, Corning, NY), each positioned with the photoreceptor side facing down and the vitreous side facing up. Excess medium was removed from the inserts, which were then placed into 6-well plates containing 1.5 ml of prewarmed complete R16 medium. The explants were incubated in a humidified CO_2 incubator at 37 °C for 24 h to allow recovery following the explantation procedure before initiating treatments. The prepared explants were then processed for downstream analyses, including PEDF/peptide treatment and immunohistochemistry.

Proteins, peptides, and inhibitors: Recombinant human PEDF[H105A], a previously reported PEDF variant that exhibits enhanced bioactivity and higher affinity for PEDF-R than native unmodified PEDF [6], was prepared as described before [22]. The peptides H105A and R99A were chemically synthesized as previously described [6], with the sequences NH_2-QRTESIIARALYYDLIS-COOH and NH_2-QATESIIHRALYYDLIS-COOH, respectively. Stock solutions of proteins and peptides were prepared in PBS or Hank's Balanced Salt Solution (HBSS) and stored at −80 °C until use. Stock solutions of atglistatin, a selective lipase inhibitor of PEDF-R/ATGL (cat. #5301510001; Millipore-Sigma), and of zaprinast, a selective inhibitor of cGMP-specific phosphodiesterases V and VI (PDE5/6; cat. #Z0878; Sigma-Aldrich, Saint Louis, MO), were prepared in dimethyl sulfoxide (DMSO) [5]. Zaprinast is about a 10-fold more potent inhibitor of PDE6 than of PDE5 [23].

Eye drop administration: For in vivo studies, 5 µl of the PEDF-derived peptide H105A (at 1 mg/ml) or vehicle (HBSS) was administered topically to the corneal surface of anesthetized mice (one eye drop per eye) as described before [13]. The contralateral eye received the vehicle as an internal control. Care was taken to ensure precise delivery and sterility during administration. Posttreatment, animals were monitored for adverse effects or signs of discomfort.

Quantitative reverse transcription polymerase chain reaction: Levels of gene transcripts in tissues were quantified using quantitative reverse transcription polymerase chain reaction (qRT-PCR). Total RNA was isolated from mouse retinas using the RNeasy Mini Kit (cat. #74104; Qiagen, Germantown, MD), following the manufacturer's instructions. RNA concentration was determined using a NanoDrop spectrophotometer (cat. #ND-ONE-W; ThermoFisher Scientific). Complementary DNA was synthesized from 500 ng total RNA using the SuperScript III First-Strand Synthesis System (cat. #18080051; Invitrogen), according to the manufacturer's protocol. qRT-PCR was performed using primers designed for *Crx* (forward: 5′-GGG GCC TCA CTA TTC AGT CA-3′; reverse: 5′-CCT CAC GTG CAT ACA CAT CC-3′) and the housekeeping gene *Rplp0* (forward: 5′-CTT CAT TGT GGG AGC AGA CA-3′; reverse: 5′-GTG AGG TCC TCC TTG GTG AA-3′; custom-purchased from Integrated DNA Technologies, Coralville, IA). The reactions were performed using the QuantiTect SYBR Green PCR Kit (cat. #204143; Qiagen), following the manufacturer's guidelines, on a QuantStudio 7 Flex thermocycler (Applied Biosystems, Foster City, CA). All qRT-PCR reactions were performed in triplicate. Relative gene expression levels were calculated using the delta-delta CT ($2^{-\Delta\Delta CT}$) method [23]. Normalization was performed by subtracting the fold change of the H105A-treated eye from the vehicle control-treated eye (HBSS, red dotted line) after normalizing gene expression to a housekeeping gene (*Rplp0*).

Histology and immunofluorescence: Enucleated eyes from mice were fixed in 10% neutral buffered formalin at 48 h (4 °C), followed by paraffin embedding, sectioning, and staining with hematoxylin and eosin as previously described [18]. To generate spider plots, the outer nuclear layer (ONL) thickness was measured from images acquired with light microscopy of the retina sections stained with hematoxylin and eosin. The ONL thickness in the entire retina sections was measured at five different positions from both sides of the optic nerve using ImageJ (National Institutes of Health, Bethesda, MD), as described before [7]. Immunofluorescence staining was performed as previously described [24]. Mouse retinas were fixed, permeabilized, and incubated with mouse primary and secondary antibodies (Table 1). For nuclear counterstaining, DAPI (1 µg/ml; cat. #MBD0015–1ML; Millipore-Sigma) or Hoechst (10 µg/ml; cat. #H3570; ThermoFisher Scientific) was employed as indicated in the figures. Retinas were mounted with photoreceptors facing up on microscope slides. Images were captured using a Zeiss LSM 880 confocal microscope (Carl Zeiss, Oberkochen, Germany) with a 63× oil immersion objective and a 1× digital zoom. Z-stacks reliably showed CRX localization restricted to the ONL. Images of Z-stacks were acquired only in regions with a detectable CRX signal, as additional stacks of unstained regions would not have provided biologically meaningful information. Because no CRX signal was observed outside the ONL in flat mounts, data from non-ONL layers were not collected, which limits quantitative assessment of background signal.

Statistics: For all in vivo and ex vivo experiments, three to four biological replicates with a minimum of three technical replicates per condition were used. Representative data for each treatment and age group were included in the analyses. Data were analyzed using GraphPad Prism (version 10.2.2; GraphPad Software, San Diego, CA). Comparisons between experimental groups were performed using unpaired/paired one- or two-tailed Student *t* tests, or ordinary one-way analysis of variance with multiple comparisons, depending on the hypothesis. Results are presented as mean ± SD, and *p* values <0.05 were considered statistically significant.

Table 1. List of antibodies.

Antibodies	Type and host	Dilution	Company, catalog number
CRX	Monoclonal, mouse	1:500	Novus Biologicals, H00001406-M02
PDE6A	Polyclonal, rabbit	1:250	Abcam, 5659
Pan-Acetylation	Monoclonal, mouse	1:250	Proteintech, 66,289-1-Ig
Alexa Fluor 488	Goat anti-Mouse	1:1000	ThermoFisher Scientific, A11029
Alexa Fluor-568	Goat anti-Rabbit	1:1000	ThermoFisher Scientific, A11036

RESULTS

Altered subcellular distribution of CRX protein in photoreceptors deficient in PEDF and PEDF-R: To examine the distribution of the CRX protein in the absence of PEDF or PEDF-R, native retinas of *Serpinf1*$^{-/-}$ or *Pnpla2*$^{-/-}$ mice, respectively, were subjected to immunofluorescence staining using wild-type mice as controls (Figure 1A). In wild-type retinas, CRX displayed a distinct and compact distribution, localized within the nuclei of photoreceptor cells, consistent with its role as a nuclear transcription factor. However, *Serpinf1*$^{-/-}$ retinas exhibited an alteration in CRX distribution. Unlike the uniform nuclear localization observed in the wild type, CRX immunolabeling in *Serpinf1*$^{-/-}$ mice was reduced (33% of wild type), appeared punctate, and was irregularly distributed throughout the photoreceptor nuclei (Figure 1B,D). In *Pnpla2*$^{-/-}$ retinas, CRX immunostaining was also significantly reduced (21% of the wild type; Figure 1C,D), with the labeling appearing fragmented, irregular, and more dispersed throughout the photoreceptor nuclei compared to wild-type retinas (Figure 1C). CRX immunolabeling of *Pnpla2*$^{-/-}$ mice exhibited a nuclear distribution pattern similar to that observed in *Serpinf1*$^{-/-}$ retinas. These findings indicate that loss of PEDF or PEDF-R alters nuclear distribution and abundance of CRX in photoreceptors, suggesting that PEDF signaling through PEDF-R contributes to proper regulation of CRX localization under physiologic conditions.

PEDF deficiency reduces PDE6A immunoreactivity and histone acetylation in photoreceptors: Because CRX regulates the expression of numerous photoreceptor genes and can promote transcription through recruitment of histone acetyltransferase–containing coactivator complexes [25], we examined PDE6A expression and pan-histone acetylation in *Serpinf1*$^{-/-}$ retinas. Immunofluorescence analysis revealed a reduction in PDE6A immunoreactivity in photoreceptors of *Serpinf1*$^{-/-}$ mice compared with wild-type controls (Figure 2A,B). Quantification of fluorescence intensity showed that PDE6A labeling was reduced by approximately 60% in *Serpinf1*$^{-/-}$ retinas relative to wild type (Figure 2B). In addition, pan-histone acetylation was significantly decreased in *Serpinf1*$^{-/-}$ photoreceptors (Figure 2A,C), with a marked reduction in fluorescence intensity compared with wild-type retinas (Figure 2C). These findings demonstrate that PEDF deficiency is associated with reduced PDE6A protein levels and decreased pan- histone acetylation in photoreceptors.

Effects of PEDF[H105A] on CRX in photoreceptor nuclei: Building on the observed differences in CRX protein

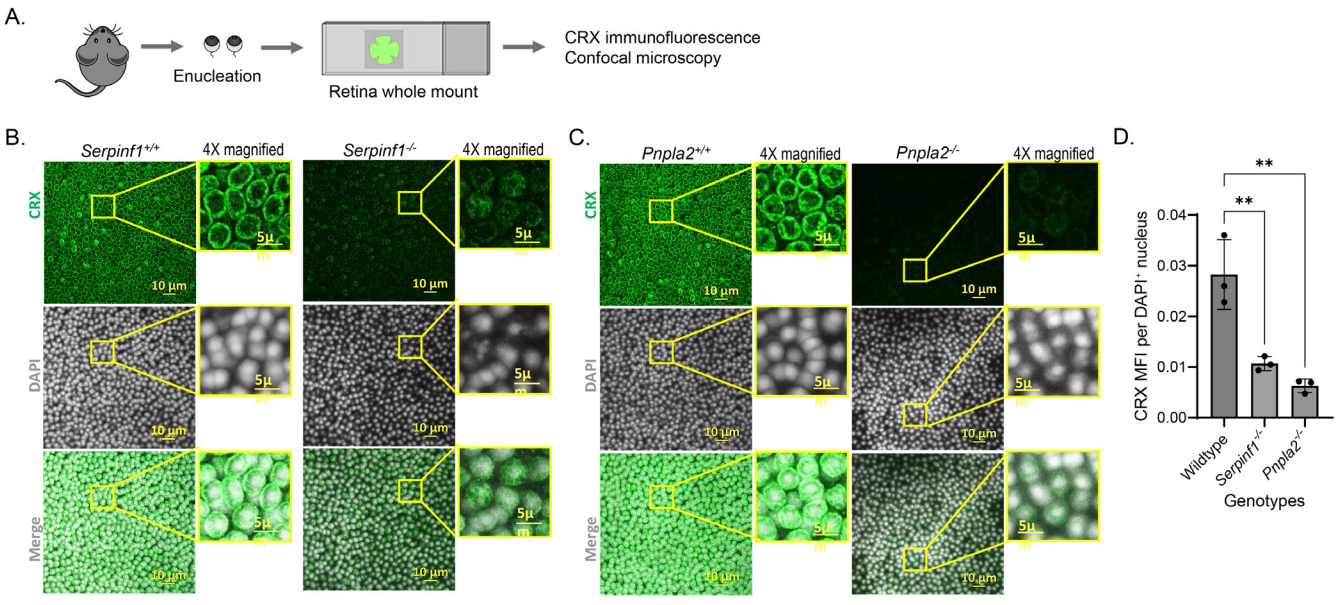


Figure 1. CRX distribution in native retinas of wild-type, *Pnpla2*$^{-/-}$, and *Serpinf1*$^{-/-}$ mice. **A**: Experimental plan. **B**: Confocal microscopy images of representative regions of interest (ROIs) showing immunostaining of CRX in whole-mount retinas of *Serpinf1*$^{+/+}$ and *Serpinf1*$^{-/-}$ mice at 3 months of age. **C**: Confocal microscopy images of representative ROIs illustrating CRX expression in whole-mount retinas from *Pnpla2*$^{+/+}$ and *Pnpla2*$^{-/-}$ mice at 3 months of age. Each image is representative of three biological replicates (mouse eye) and four technical replicates (ROIs per eye). **D**: CRX mean fluorescence intensity (MFI) was measured within each ROI and normalized to the number of DAPI-positive nuclei; each point represents one explant from one of three independent mice (n = 3). Data are shown as mean ± SD. Statistical significance was determined by ordinary one-way analysis of variance multiple comparisons: **p < 0.01.

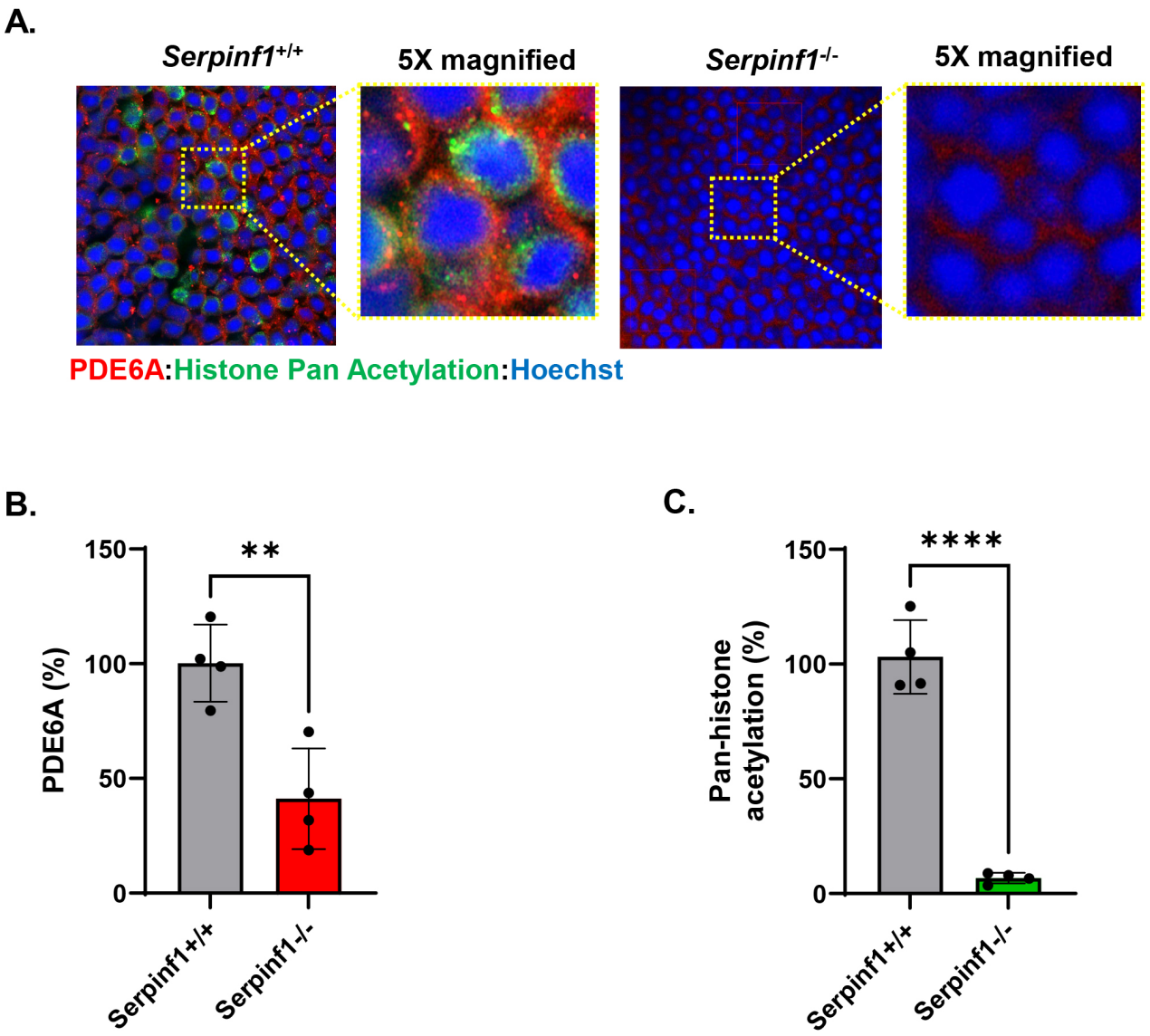


Figure 2. Reduced PDE6A immunoreactivity and pan-histone acetylation in photoreceptors of *Serpinf1*$^{-/-}$ mice. **A**: Representative regions of interest (ROIs) from *Serpinf1*$^{+/+}$ and *Serpinf1*$^{-/-}$ retinas showing PDE6A immunoreactivity (red), pan-histone acetylation (green), and Hoechst nuclear staining (blue) by confocal microscopy. Regions indicated by yellow squares are shown at higher magnification. **B**: Quantification of PDE6A mean fluorescence intensity (MFI). **C**: Quantification of pan-histone acetylation MFI. Quantification was performed using two ROIs from of three biological replicates. Mice were 3 months old. *p < 0.05, **p < 0.01.

distribution between photoreceptors of wild-type and *Serpinf1*$^{-/-}$ mice, we investigated whether the PEDF[H105A] protein, a PEDF variant containing the H105A substitution, could restore CRX within photoreceptor nuclei. PEDF[H105A] was chosen due to its higher binding affinity for PEDF-R and enhanced bioactivity compared to unmodified PEDF [6]. Retinal explants from wild-type mice were cultured and treated with PEDF[H105A] protein (Figure 3A). CRX protein distribution and relative signal intensity were assessed in whole-mount retinas by immunofluorescence. In untreated explants, there was a reduction in photoreceptor nuclei, with the remaining nuclei appearing shrunken (Figure 3B), consistent with photoreceptor distress under ex vivo culture conditions.

In contrast, PEDF[H105A]-treated retinas exhibited preserved nuclear morphology and maintained

CRX localization in a ring-like pattern (Figure 3B). The PEDF[H105A] treatment increased the CRX immunolabel intensity to sixfold relative to untreated retinas (Figure 3C).

Statistical analysis showed no significant difference in CRX intensity/DAPI between freshly isolated wild-type retinas and retinal explants treated with PEDF[H105A] (p = 0.326), and CRX levels in PEDF[H105A]-treated explants were comparable to those observed in freshly isolated retinas.

In addition, PEDF treatment increased the expression of *Crx* and several photoreceptor-associated genes, including *Pde6a*, *Pde6b*, *Opn1mw*, *Opn1sw*, and *Arr3*, in retinal explants (Appendix 1). These findings complement the increase in CRX protein levels and support the ability of PEDF signaling to promote transcriptional programs associated with photoreceptor function. In contrast, neither PEDF treatment nor *Serpinf1* deletion significantly altered *Nrl* or *Nr2e3* transcript levels in retinal explants or mouse retinas,

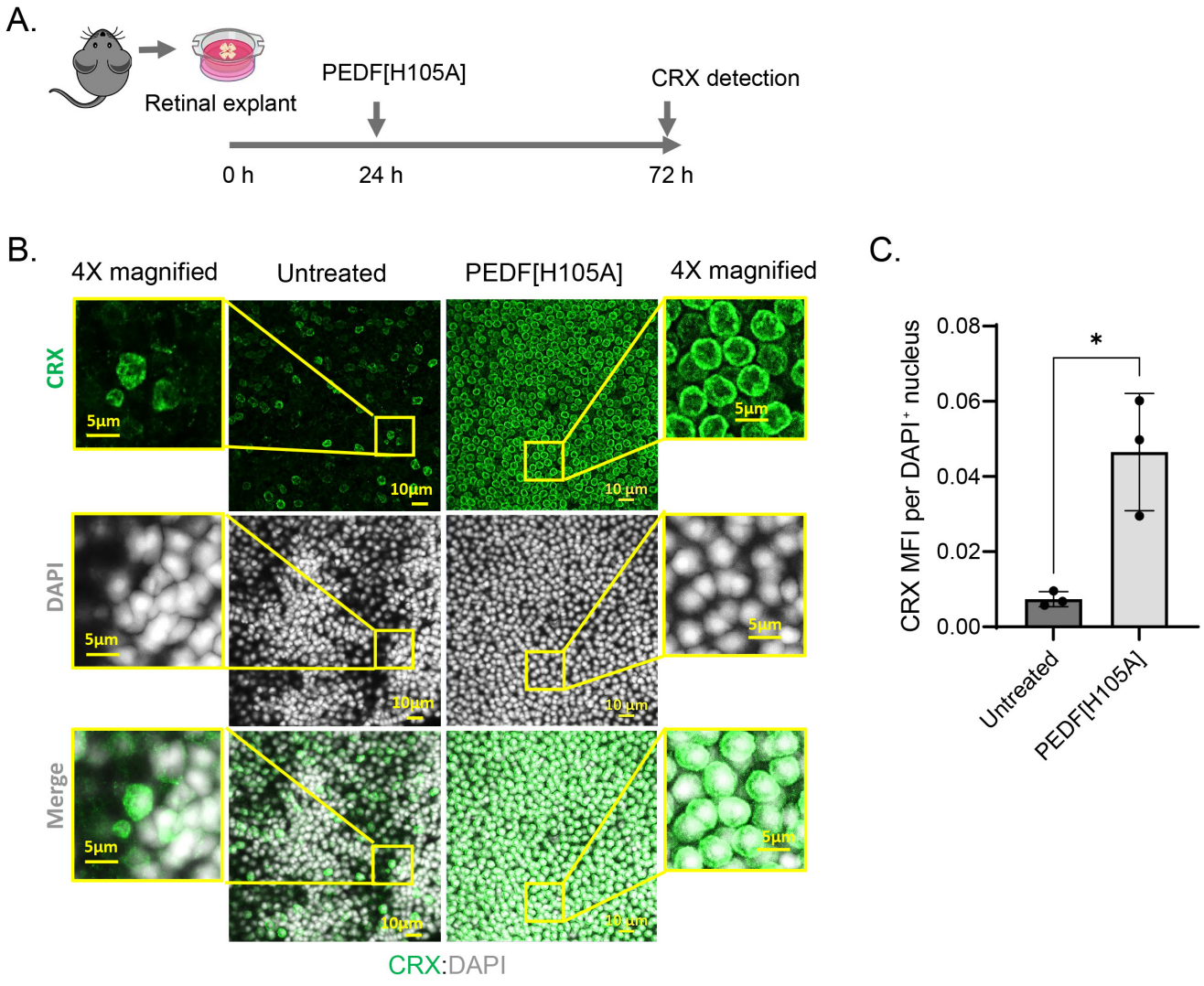


Figure 3. Effects of PEDF[H105A] protein on CRX in mouse photoreceptors. **A**: Treatment scheme illustrating wild-type mouse retinal explants treated without or with 20 nM PEDF[H105A] for 48 h. **B**: Representative regions of interest (ROIs) from confocal microscopy images of the retinal explants with CRX immunofluorescence staining (green) and DAPI staining of photoreceptor nuclei (pseudo-gray). Data are representative of three biological replicates (three eyes) and four technical replicates (ROIs per eye). Mice were 3 months old. **C**: CRX mean fluorescence intensity (MFI) was measured within each ROI and normalized to the number of DAPI-positive nuclei; each point represents one explant from one of three independent mice (n = 3). Data are shown as mean ± SD. Statistical significance was determined by an unpaired *t* test: *p < 0.05.

respectively (Appendix 2). These findings demonstrate that PEDF[H105A] protein preserves the CRX signal in photoreceptor nuclei under ex vivo conditions in retinal explants.

Restoration of CRX in photoreceptors undergoing zaprinast-induced degeneration by PEDF[H105A]: Previously, we demonstrated that zaprinast, a phosphodiesterase V/VI (PDE5/6) inhibitor, induces photoreceptor cell death and that PEDF mitigates this degeneration [5]. To further explore the relationship between CRX expression and photoreceptor degeneration, retinal explants were pretreated with PEDF[H105A], followed by exposure to zaprinast, as described in Figure 4A. Zaprinast significantly reduced CRX immunoreactivity normalized to DAPI (to 61% relative to explants without zaprinast) and altered its spatial distribution in wild-type retinas, resulting in a more dispersed and irregular CRX pattern (Figure 4B,C). In contrast, PEDF[H105A] pretreatment preserved CRX immunoreactivity, yielding levels comparable to controls (100% relative to explants without zaprinast and 163% relative to explants with zaprinast), with more compact nuclear distribution in photoreceptors (Figure 4C). Photoreceptor cell death was additionally assessed using PSVue-550 staining in retinal explants (Appendix 3). Zaprinast treatment increased the proportion of PSVue-positive photoreceptors, whereas PEDF treatment reduced photoreceptor cell death in both *Serpinf1*$^{+/+}$ and *Serpinf1*$^{-/-}$ retinal explants. These findings are consistent with the previously reported neuroprotective effects of PEDF and PEDF-derived peptides in retinal degeneration models [5,6,13].

These findings indicate that PEDF[H105A] maintains CRX signal under both baseline and zaprinast-induced conditions in photoreceptors in retinal explants.

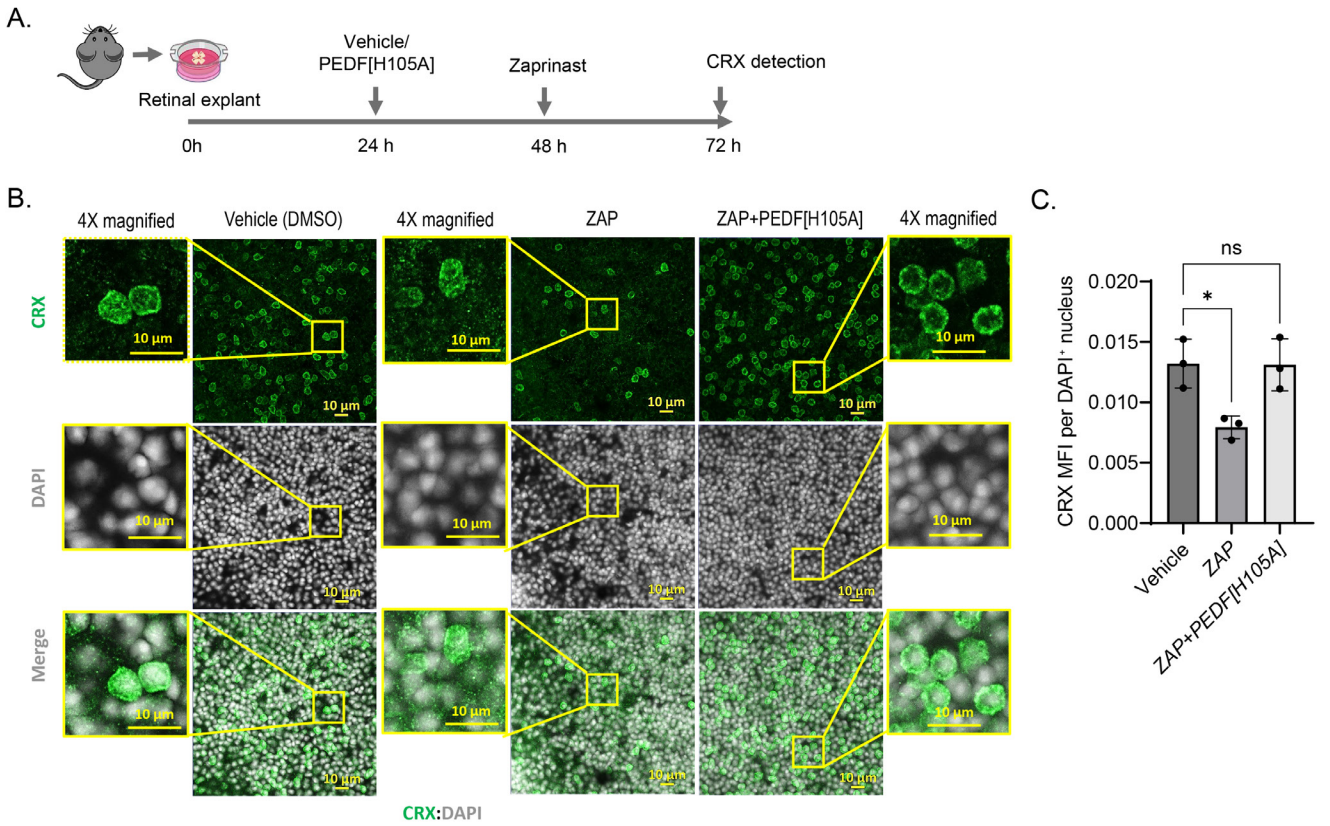


Figure 4. PEDF effects on CRX in the nuclei of photoreceptors undergoing zaprinast-induced degeneration. **A**: Schematic illustration of the treatment protocol of wild-type mouse retinal explants without or with 20 nM PEDF[H105A] protein, followed by 100 µM zaprinast addition. **B**: Representative confocal microscopy images of retinal explants showing CRX immunofluorescence staining (green) and DAPI staining of photoreceptor nuclei (pseudo-gray). Retinas were treated with vehicle (equivalent volumes of DMSO and PBS), PEDF[H105A] (20 nM), and zaprinast (100 µM). Data are representative of four biological replicates (n = 4 eyes) with four technical replicates (ROIs per eye) per condition. Mice were 3 months old. **C**: CRX mean fluorescence intensity (MFI) was measured within each ROI and normalized to the number of DAPI-positive nuclei; each point represents one explant from one of three independent mice (n = 3). Data are shown as mean ± SD. Statistical significance was determined by ordinary one-way analysis of variance multiple comparisons: ns, not significant; *p < 0.05.

Increased Crx expression in rd10 and rd10/Serpinf1$^{-/-}$ mouse retinas by H105A peptide: The H105A peptide is a small peptide of 17 amino acid residues from the receptor-binding domain of PEDF with a single alteration at position 105 of the human PEDF sequence from histidine to alanine [6]. It has higher binding affinity for PEDF-R than the unmodified 17-mer peptide, is bioactive, and replicates the neurotrophic signaling cascade observed with the full-length PEDF protein [6,12]. Previous studies showed that daily administration of the H105A peptide via eye drops for 1 week, starting at P15—before the peak of photoreceptor death peak—delayed photoreceptor degeneration and promoted survival in *rd10* and *rd10/Serpinf1*$^{-/-}$ mice [13].

We determined *Crx* transcript expression in retinas of *rd10* and *rd10/Serpinf1*$^{-/-}$ mice at P15. Quantification of *Crx* transcript levels showed a reduction in both *rd10* and *rd10/Serpinf1*$^{-/-}$ retinas compared to wild-type controls (Appendix 4). This reduction correlated with decreases in ONL thickness relative to wild-type (Appendix 4), suggesting that reduced *Crx* expression may result from photoreceptor loss in the mutated mice. To evaluate the effects of exogenous H105A peptide on *Crx* transcript levels, a single dose of H105A peptide (5 µg/eye) was administered via eye drops to *rd10* and *rd10/Serpinf1*$^{-/-}$ mice at P15 (Figure 5A). *Crx* transcript levels in retinal tissues assessed at 1, 3, 6, and 24 h after eye drop administration show that at 1 h posttreatment, H105A peptide upregulated *Crx* mRNA levels in both *rd10* and *rd10/Serpinf1*$^{-/-}$ retinas compared with vehicle controls (Figure 5B). However, *Crx* expression returned to baseline by 3 h and remained unchanged at 6 and 24 h. These findings indicate that H105A, the PEDF-R binding peptide, elicits a rapid but transient increase in *Crx* gene expression in vivo, reinforcing its role as a modulator of CRX expression in photoreceptors.

PEDF-R binding requirement for CRX regulation: To examine the role of the PEDF-R in PEDF-induced CRX expression, retinal explant cultures from wild-type mice were treated with the neurotrophic H105A peptide (Figure 6A). As a negative control, we used the R99A peptide, a variant lacking PEDF-R binding affinity and neurotrophic activity. PEDF[H105A] protein (with the H105A substitution identical to the H105A peptide) served as a positive control.

Treatment with the H105A peptide (20 nM) significantly increased CRX protein levels (190% of the explants without peptide) with compact distribution in photoreceptor nuclei (Figure 6B,C). Nuclear morphology was also preserved in treated explants, as confirmed by DAPI staining. Similar effects were observed with PEDF[H105A] protein compared with untreated explants, with an increase of 270% relative to untreated controls (Figure 6C). In contrast, R99A-treated explants displayed structural degeneration, including large gaps in whole-mount preparations, reduced CRX immunolabeling, and disrupted nuclear morphology, and CRX distribution. These results demonstrate that PEDF-R binding is essential for PEDF-mediated upregulation of CRX as well as for its neuroprotective effects on photoreceptors.

PEDF-R activity requirement for PEDF-mediated CRX expression: To investigate the role of PEDF-R enzymatic activity in CRX regulation, we used atglistatin, a selective and competitive inhibitor of the enzymatic activity of PEDF-R/adipose triglyceride lipase (ATGL) lipase activity. Previous studies have shown that atglistatin inhibits the cytoprotective effects mediated by H105A in retinal R28 cells [6]. In the present study, wild-type retinal explants were incubated with atglistatin in combination with the H105A peptide (Figure 7A) to determine whether atglistatin inhibits H105A-induced CRX regulation. Figure 7B shows that atglistatin completely abolished H105A-induced CRX expression and annular distribution in the nucleus, whereas no effect was observed with vehicle-treated (DMSO) controls or atglistatin by itself. CRX immunolabel intensity was 85% for atglistatin alone, 92% with H105A + atglistatin, and 185% with only H105A treatment relative to vehicle (Figure 7C). These findings demonstrate that H105A-mediated modulation of CRX specifically depends on the enzymatic activity of PEDF-R.

DISCUSSION

Our findings show that PEDF treatment leads to increased CRX immunoreactivity and a more organized nuclear distribution, supporting a contributory role for CRX in the neurotrophic response of photoreceptors. This is in line with the established role of CRX in photoreceptor maintenance and survival. Several findings support this conclusion. CRX upregulation was greater in wild-type than in PEDF-deficient mouse retinas and was further enhanced by treatment with the PEDF[H105A] protein or H105A peptide. These effects were observed in retinas in vivo, in neural retinal explants without RPE ex vivo, and under conditions of PDE6 inhibition (using zaprinast) or *Pde6b* mutation (e.g., *rd10* models). Additionally, the results confirmed that PEDF ligand–receptor interactions and the PEDF-R phospholipase activities are essential for these processes. Collectively, these findings support the notion that CRX participates in PEDF-mediated signaling pathways associated with photoreceptor survival and provide new insight into how PEDF may modulate CRX expression in the degenerating retina.

To our knowledge, this study is the first to demonstrate that both binding and stimulation of PEDF-R phospholipase activity by PEDF are necessary for CRX upregulation. This

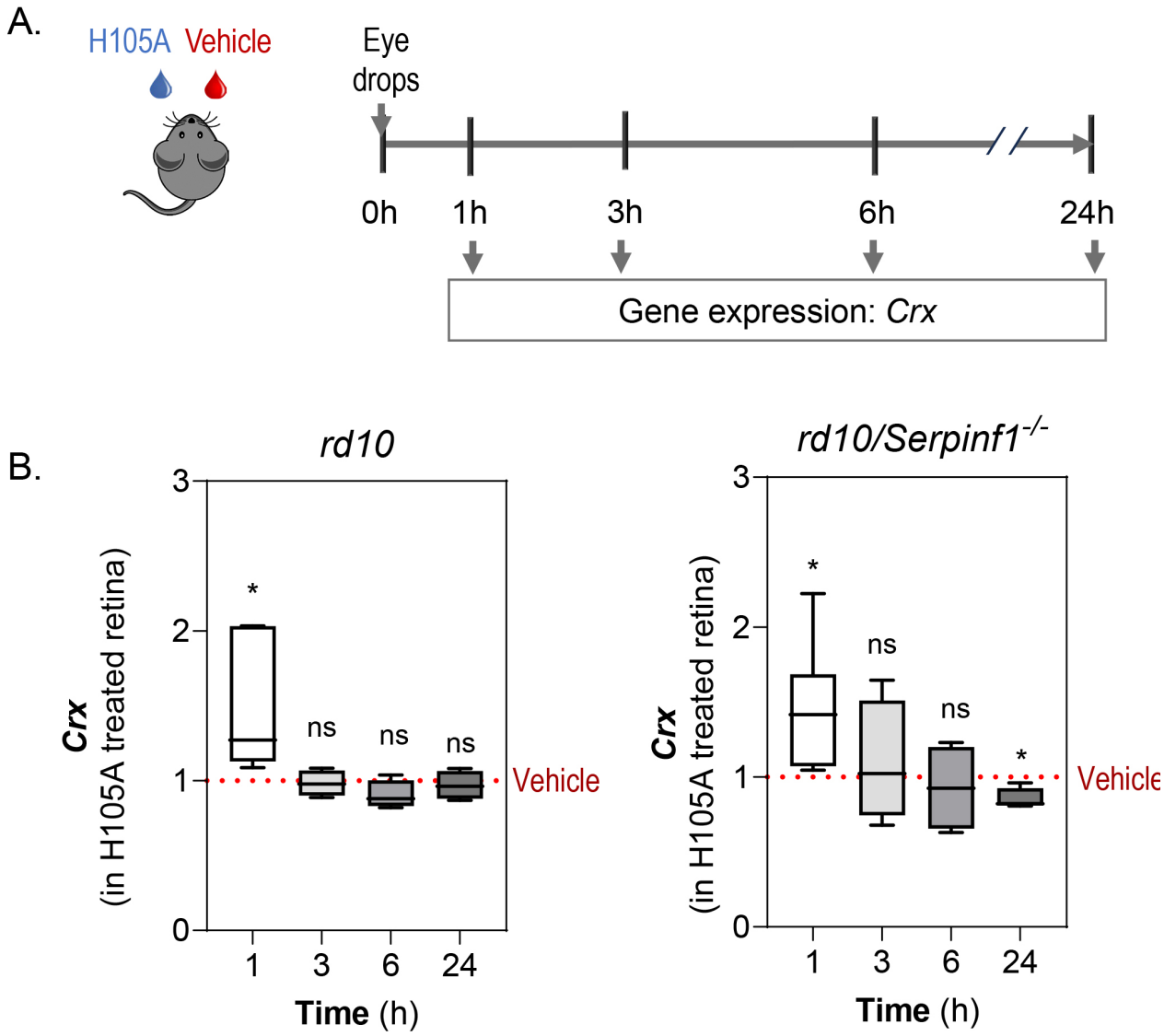


Figure 5. *Crx* gene expression in retinas of mice treated with H105A peptide eye drops. **A**: Scheme of the experimental plan. *rd10* and *rd10/Serpinf1*$^{-/-}$ mice (at postnatal day 15) were treated with a single 5-µl eye drop of H105A (left eye; 1 mg/ml) or vehicle control (right eye; HBSS). After 1, 3, 6, and 24 h of eye drop administration, mice were euthanized, and retinas were dissected and subjected to qRT-PCR to detect *Crx* gene expression. **B**: Plots of time-dependent changes in *Crx* mRNA levels using a box-and-whisker plot. Fold change was calculated using three quantitative PCR replicates from four independent biological replicates (eyes). The effects of the vehicle control (HBSS) are indicated by the red dotted line on the graph. Statistical analysis was performed using GraphPad Prism, version 10.2.2 (397). ns, not significant; *p < 0.04.

effect was replicated by the neurotrophic peptide H105A in retinal explants and live mice, underscoring the role of the PEDF/PEDF-R axis in photoreceptor homeostasis through CRX regulation. CRX is a transcription factor that drives the expression of genes critical for phototransduction and outer segment maintenance, such as *Pde6* [26,27]. Accordingly, PEDF ablation in *Serpinf1*$^{-/-}$ mice resulted in reduced nuclear CRX distribution, lower PDE6A levels, and decreased pan-histone acetylation in photoreceptors (Figure 2), findings that are consistent with diminished CRX-dependent transcriptional regulation in the absence of PEDF [25]. To further explore the role of PEDF in modulating CRX-driven transcriptional programs, we analyzed the expression of several established CRX target genes in retinal explants treated with

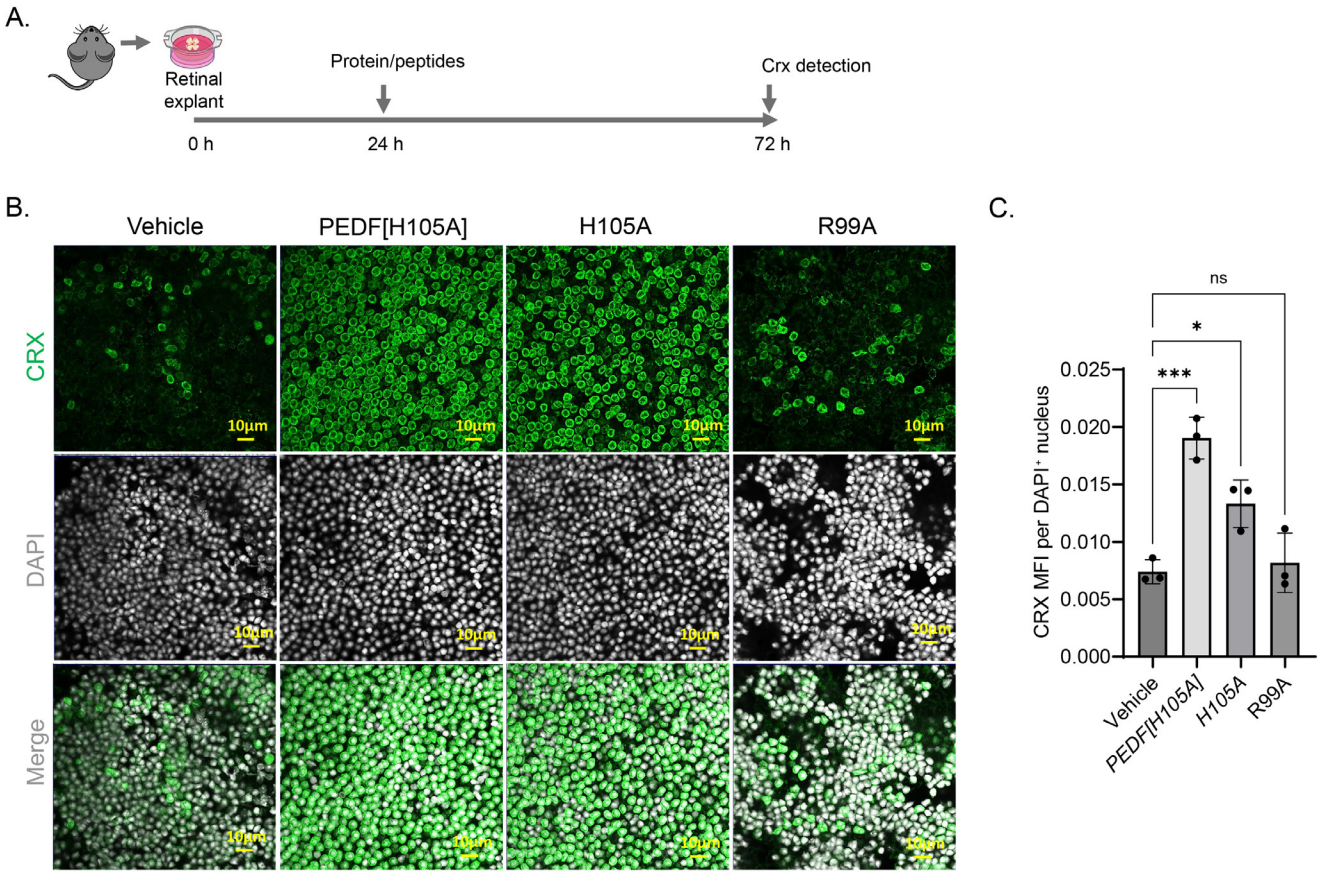


Figure 6. Effects of PEDF-R–binding peptides on CRX in photoreceptors. **A**: Schematic illustration of the treatment protocol of wild-type mouse retinal explants with PBS (vehicle) or 20 nM of each PEDF[H105A] (positive control), H105A peptide, and R99A peptide (negative control) for 48 h followed by CRX detection. **B**: Representative regions of interest (ROIs) from confocal microscopy images of retinal explant cultures. Three biological replicates (three eyes) were used for each vehicle and PEDF[H105A] treatment, while four biological replicates (4 eyes) were used for the R99A and H105A groups. Each condition included four technical replicates (ROIs). Mice were 3 months old. **C**: CRX mean fluorescence intensity (MFI) was measured within each ROI and normalized to the number of DAPI-positive nuclei; each point represents one explant from one of three independent mice (n = 3). Data are shown as mean ± SD. Statistical significance was determined by ordinary one-way analysis of variance multiple comparisons: ns, not significant; *p < 0.05, ***p < 0.001.

PEDF for 24 and 48 h. PEDF treatment led to upregulation of *Crx* itself, along with key photoreceptor-specific genes such as *Pde6a*, *Pde6b*, *Opn1mw*, *Opn1sw*, and *Arr3*, all of which are known CRX targets (Appendix 1). Notably, PEDF also induced *Bcl2*, a pro-survival gene previously associated with PEDF signaling [9], although it is not directly regulated by CRX. These findings are consistent with PEDF enhancing CRX-mediated transcriptional programs. Previous reports describing PEDF-mediated photoreceptor survival [1–3,5,6,8] (Appendix 3) further support a role for PEDF/PEDF-R signaling in photoreceptor biology. The transient increase in *Crx* expression observed after topical administration of H105A differs from the sustained response observed in retinal explants. These differences likely reflect distinct pharmacokinetic and pharmacodynamic conditions in the intact eye versus organotypic culture systems. Eye drop administration results in transient retinal exposure, whereas explants are continuously exposed to the ligand in culture, enabling sustained transcriptional responses at later time points. CRX protein levels were not assessed following topical administration; therefore, it remains unknown whether transcriptional changes translate into corresponding protein-level changes. Further studies will be required to determine protein-level responses under this experimental paradigm.

Similarly, PEDF-R deficiency in *Pnpla2*$^{-/-}$ mice mirrored these alterations, further underscoring the critical roles of PEDF and PEDF-R in maintaining CRX nuclear distribution and its potential function in photoreceptors. In contrast, PEDF treatment or genetic deletion of *Serpinf1* did not alter *Nrl* and *Nr2e3* transcript levels in mouse retinas (Appendix 2).

Because NRL and NR2E3 function together with CRX in the transcriptional regulation of photoreceptor genes, these findings suggest that PEDF signaling selectively affects CRX-associated pathways without broadly altering the expression of other key photoreceptor transcription factors [15,28].

PEDF has been reported to reduce intracellular calcium levels in degenerating retinas, including in models of PDE6 mutation such as *rd1* and *rd10*, where disrupted calcium homeostasis is a hallmark of photoreceptor degeneration [12,29,30]. Calcium is a key regulator of multiple cellular processes, including nuclear signaling, transcription factor activity, and chromatin structure [31–33]. In this context, calcium dysregulation represents an important feature of photoreceptor degeneration that may be modulated indirectly by neuroprotective signaling pathways such as those triggered by PEDF. However, the present study does not directly assess calcium signaling, and any connection between PEDF-mediated CRX regulation and calcium-dependent nuclear processes remains speculative.

A potential link between the PEDF/PEDF-R signaling and nuclear lipid homeostasis is also proposed. PEDF-R is a key enzyme involved in lipid metabolism and signaling in photoreceptors [10,11]. Deletion of the gene encoding PEDF-R (*Pnpla2*) leads to photoreceptor degeneration and the accumulation of lysophosphatidylcholine– docosahexaenoic acid (DHA) and lysophosphatidylethanolamine–DHA [18], highlighting a connection between lipid imbalances and photoreceptor dysfunction. PEDF stimulation of the lipase activity of PEDF-R at the plasma or the nuclear envelope membranes may serve as an upstream mechanism. Although PEDF

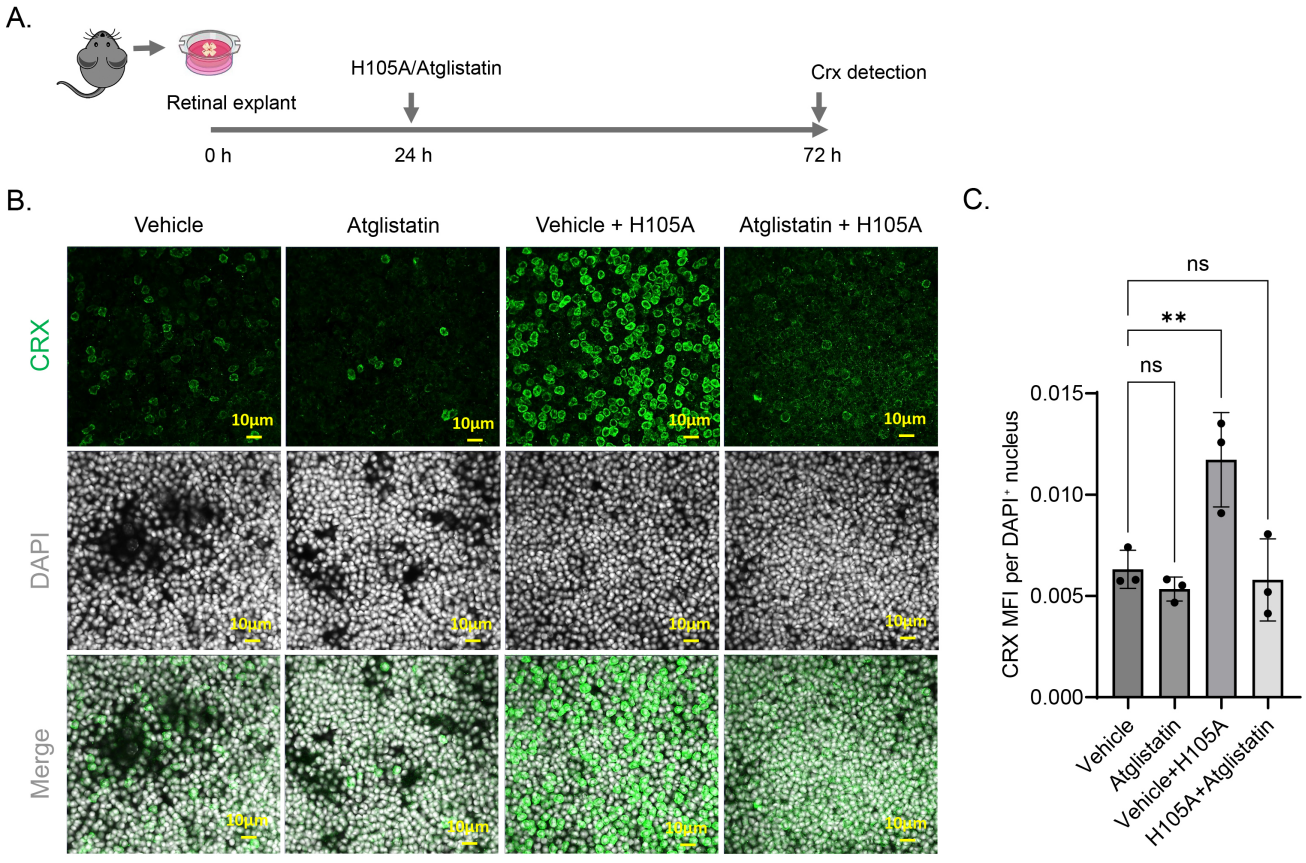


Figure 7. Effects of PEDF-R inhibition on CRX expression. **A**: Schematic illustration of the treatment protocol of wild-type mouse retinal explants with vehicle (DMSO), atglistatin (100 µM), H105A peptide (20 nM), or a combination of atglistatin and H105A for 48 h followed by CRX detection. **B**: Representative images of regions of interest (ROIs) of treated retinal explants. Images are representative of four technical replicates (ROIs) and four biological replicates (eyes) per condition. Mice were 3 months old. **C**: CRX mean fluorescence intensity (MFI) was measured within each ROI and normalized to the number of DAPI-positive nuclei; each point represents one explant from one of three independent mice (n = 3). Data are shown as mean ± SD. Statistical significance was determined by ordinary one-way analysis of variance multiple comparisons: ns, not significant; **p < 0.01.

is an extracellular protein, it has been detected in nuclear membranes [34], and PEDF-R localizes to both plasma and nuclear membranes [10,35–39]. Upon PEDF binding, PEDF-R catalyzes the release of fatty acids and lysophospholipids from phospholipids, which could translocate into the nucleus to regulate gene expression, including *Crx*. This mechanism aligns with emerging research on the roles of nuclear lipids in transcription factor activity, RNA synthesis, and cellular processes such as proliferation, differentiation, and apoptosis, particularly in the nervous system and in ocular tissues [38–40].

It is important to note that species-specific differences in CRX-dependent regulatory networks have been reported. Bibb and colleagues [41] demonstrated key differences between human and mouse retinal development, including differences in the timing of CRX expression relative to the expression of photoreceptor genes, such as those encoding PDE6B and arrestin. These findings suggest that developmental regulatory programs involving CRX are not fully conserved between species and that caution is warranted when extrapolating developmental mechanisms from mouse models to humans. However, the present study focuses on CRX regulation in the mature retina rather than during development. Whether PEDF/PEDF-R signaling also regulates CRX in the adult human retina remains to be determined.

Because CRX regulates a broad network of photoreceptor genes involved in phototransduction and cellular maintenance, modulation of CRX through PEDF/PEDF-R signaling may provide the basis for a potential gene-agnostic approach to support photoreceptor function and homeostasis. Unlike mutation-specific strategies, enhancement of endogenous neuroprotective pathways could be beneficial across multiple forms of retinal degeneration. However, additional studies are required to determine whether PEDF-mediated regulation of CRX contributes directly to long-term photoreceptor preservation in diverse models of retinitis pigmentosa.

Future research is needed to delineate the molecular pathways linking PEDF and PEDF-R enzymatic activity to CRX expression, localization, and function. Understanding these pathways could reveal new therapeutic targets for preserving photoreceptor health and preventing degeneration. While our findings demonstrate that PEDF modulates CRX expression and localization in adult explants, whether PEDF exerts similar regulatory effects during retinal development remains to be determined.

In conclusion, this study highlights the critical role of PEDF, mediated through PEDF-R, in maintaining CRX homeostasis, supporting transcriptional activity of CRX and pathways associated with photoreceptor integrity and function. These findings provide a strong foundation for developing therapies to preserve vision in retinal degenerative diseases.

APPENDIX 1. SUPPLEMENTAL FIGURE 1.

To access the data, click or select the words "Appendix 1." PEDF treatment induced the expression of Crx and Pde6a, Pde6b, Opn1mw, Opn1sw and Arr3 in retinal explants. Wild-type mouse retinal explants were treated with PEDF for the indicated times (see x-axis). Fold change was calculated using 3 qPCR replicates from 3 independent biological replicates. Normalization was performed subtracting the fold change of PEDF treatment from the control (untreated) retinal explants (red line in the graph), after normalizing gene expression to a housekeeping gene (Rplp0). Fold change 1 = no change. P-values vs the untreated control are shown: ns, not significant, * $p < 0.05$; ** $p < 0,01$; *** $p < 0.001$.

APPENDIX 2. SUPPLEMENTAL FIGURE 2.

To access the data, click or select the words "Appendix 2." Nrl and Nr2e3 expression in retina and retinal explants. Exogenous PEDF treatment and genetic deletion of *Serpinf1* do not alter *Nrl* and *Nr2e3* transcript levels in mouse retina. (A-B) Quantitative reverse transcription PCR (qRT-PCR) analysis of *Nrl* (panel A) and *Nr2e3* (panel B) mRNA levels under two conditions: (1) retinal explants from wild-type (Serpinf1+/+) mice (3 months old) treated with or without 20 nM recombinant PEDF for 48 hours, and (2) freshly isolated retinas from Serpinf1+/+ and Serpinf1-/- mice at postnatal day 15 (P15). Fold-change values were calculated from three qPCR technical replicates per sample, using two biological replicates for explant cultures and three biological replicates for fresh retinal tissues. ns=not significant.

APPENDIX 3. SUPPLEMENTAL FIGURE 3.

To access the data, click or select the words "Appendix 3." Ex vivo protection of photoreceptor cells against death induced by Zaprinast. Explants were treated as illustrated at the top. Cell death was followed by phosphatidyl serine externalization using PSVue-550, as described before [12] A. Representative images of ROIs each from Serpinf1+/+ and Serpinf1-/- retinal explants under different treatments showing photoreceptors nuclei (Hoechst, blue) and PSVue-550 (red) by confocal super resolution microscopy. B. Quantification of PSVue-550 detection normalized to the number of Hoechst-stained nuclei corresponding to photoreceptor (PR), corresponding to a total of 2 ROIs per 2 biological replicates. PEDF protected photoreceptor cells against death induced by Zaprinast ex vivo. Serpinf1-/- retinas were more susceptible

to retinal degeneration and PEDF treatment decreased the portion of PSVue-positive photoreceptors in both Serpinf1+/+ and Serpinf1-/- retinal explants.

APPENDIX 4. SUPPLEMENTAL FIGURE 4.

To access the data, click or select the words "Appendix 4." rd10 and rd10/Serpinf1-/- mice exhibited low Crx expression as compared to Wildtype mice rd10 and rd10/Serpinf1-/- mice exhibited low Crx expression as compared to wild type (WT) mice. (A) Retinas were isolated from WT, Serpinf1-/-, rd10 and rd10/Serpinf1-/- mice at post-natal day 15 (P15) and qRT-PCR was performed to determine Crx mRNA levels. Fold-change was calculated using three (3) qPCR replicates from four (4) independent biological replicates (eyes). (B) Spider plot analysis illustrating outer nuclear layer (ONL) thickness in all four genotypes. (C) Representative images of retina sections of WT, Serpinf1-/-, rd10 and rd10/Serpinf1-/- mice at P15 stained with hematoxylin and eosin. Statistical analysis was performed using GraphPad Prism. ns=not significant, **< 0.0044, ***< 0. 0.0009.

ACKNOWLEDGMENTS

This research was supported by the Intramural Research Program of the National Institutes of Health (NIH; Project #ZIAEY000306, SPB). The contributions of the NIH authors were made as part of their official duties as NIH federal employees, are in compliance with agency policy requirements, and are considered Works of the United States Government. However, the findings and conclusions presented in this paper are those of the authors and do not necessarily reflect the views of the NIH or the USA Department of Health and Human Services. Confocal super resolution images were generated in the Bioimaging Core Facility, and hematoxylin and eosin staining at Histology core at NEI-NIH. We thank Ms. Megan Kopera and Ms. Alexandra Bernardo-Colón for assistance with mouse breeding and animal care, Dr. Debnath for purifying PEDF[H105A] protein and Miss Paige Chambers and Ms. Alexandra Bernardo-Colon for performing immunofluorescence on retinal cross sections. Commercial relationships disclosures: S. Dixit, None; I.T. Rebustini, none; SEM. Crawford, none; S.P. Becerra, None. Prior presentations: ARVO 2023, NIH Research Festival 2023.

This is an open-access article distributed under the terms of the Creative Commons Attribution-NonCommercial-NoDerivatives 4.0 International License, which permits reusers to copy and distribute the material in any medium or format in unadapted form only, for noncommercial purposes only, and only so long as attribution is given to the creator. CC BY-NC-ND includes the following elements: BY: credit must be given to the creator. NC: Only noncommercial uses of the work are permitted. ND: No derivatives or adaptations of the work are permitted.

REFERENCES

1. Pagan-Mercado G, Becerra SP. Signaling Mechanisms Involved in PEDF-Mediated Retinoprotection. Adv Exp Med Biol 2019; 1185:445-9. [PMID: 31884652].
2. Polato F, Becerra SP. Pigment Epithelium-Derived Factor, a Protective Factor for Photoreceptors in Vivo. Adv Exp Med Biol 2016; 854:699-706. [PMID: 26427478].
3. Cayouette M, Smith SB, Becerra SP, Gravel C. Pigment epithelium-derived factor delays the death of photoreceptors in mouse models of inherited retinal degenerations. Neurobiol Dis 1999; 6:523-32. [PMID: 10600408].
4. Chang B, Hawes NL, Pardue MT, German AM, Hurd RE, Davisson MT, Nusinowitz S, Rengarajan K, Boyd AP, Sidney SS, Phillips MJ, Stewart RE, Chaudhury R, Nickerson JM, Heckenlively JR, Boatright JH. Two mouse retinal degenerations caused by missense mutations in the beta-subunit of rod cGMP phosphodiesterase gene. Vision Res 2007; 47:624-33. [PMID: 17267005].
5. Hernández-Pinto A, Polato F, Subramanian P, Rocha-Muñoz A, Vitale S, de la Rosa EJ, Becerra SP. PEDF peptides promote photoreceptor survival in rd10 retina models. Exp Eye Res 2019; 184:24-9. [PMID: 30980815].
6. Kenealey J, Subramanian P, Comitato A, Bullock J, Keehan L, Polato F, Hoover D, Marigo V, Becerra SP. Small Retinoprotective Peptides Reveal a Receptor-binding Region on Pigment Epithelium-derived Factor. J Biol Chem 2015; 290:25241-53. [PMID: 26304116].
7. Dixit S, Polato F, Samardzija M, Abu-Asab M, Grimm C, Crawford SE, Becerra SP. PEDF deficiency increases the susceptibility of rd10 mice to retinal degeneration. Exp Eye Res 2020; 198:108121[PMID: 32721425].
8. Murakami Y, Ikeda Y, Yonemitsu Y, Onimaru M, Nakagawa K, Kohno R, Miyazaki M, Hisatomi T, Nakamura M, Yabe T, Hasegawa M, Ishibashi T, Sueishi K. Inhibition of nuclear translocation of apoptosis-inducing factor is an essential mechanism of the neuroprotective activity of pigment epithelium-derived factor in a rat model of retinal degeneration. Am J Pathol 2008; 173:1326-38. [PMID: 18845835].
9. Bazan HEP, Pham TL. A new R,R-RvD6 isomer with protective actions following corneal nerve injury. Prostaglandins Other Lipid Mediat 2024; 170:106802[PMID: 38036037].
10. Notari L, Baladron V, Aroca-Aguilar JD, Balko N, Heredia R, Meyer C, Notario PM, Saravanamuthu S, Nueda ML, Sanchez-Sanchez F, Escribano J, Laborda J, Becerra SP. Identification of a lipase-linked cell membrane receptor for pigment epithelium-derived factor. J Biol Chem 2006; 281:38022-37. [PMID: 17032652].
11. Subramanian P, Locatelli-Hoops S, Kenealey J, DesJardin J, Notari L, Becerra SP. Pigment epithelium-derived factor

(PEDF) prevents retinal cell death via PEDF Receptor (PEDF-R): identification of a functional ligand binding site. J Biol Chem 2013; 288:23928-42. [PMID: 23818523].

12. Comitato A, Subramanian P, Turchiano G, Montanari M, Becerra SP, Marigo V. Pigment epithelium-derived factor hinders photoreceptor cell death by reducing intracellular calcium in the degenerating retina. Cell Death Dis 2018; 9:560-[PMID: 29752430].

13. Bernardo-Colón A, Bighinati A, Parween S, Debnath S, Piano I, Adani E, Corsi F, Gargini C, Vergara N, Marigo V, Patricia Becerra S. H105A peptide eye drops promote photoreceptor survival in murine and human models of retinal degeneration. Commun Med (Lond) 2025; 5:81-[PMID: 40118996].

14. Furukawa T, Morrow EM, Cepko CL. Crx, a novel otx-like homeobox gene, shows photoreceptor-specific expression and regulates photoreceptor differentiation. Cell 1997; 91:531-41. [PMID: 9390562].

15. Swaroop A, Kim D, Forrest D. Transcriptional regulation of photoreceptor development and homeostasis in the mammalian retina. Nat Rev Neurosci 2010; 11:563-76. [PMID: 20648062].

16. Kruczek K, Qu Z, Gentry J, Fadl BR, Gieser L, Hiriyanna S, Batz Z, Samant M, Samanta A, Chu CJ, Campello L, Brooks BP, Wu Z, Swaroop A. Gene Therapy of Dominant CRX-Leber Congenital Amaurosis using Patient Stem Cell-Derived Retinal Organoids. Stem Cell Reports 2021; 16:252-63. [PMID: 33513359].

17. Roger JE, Hiriyanna A, Gotoh N, Hao H, Cheng DF, Ratnapriya R, Kautzmann MA, Chang B, Swaroop A. OTX2 loss causes rod differentiation defect in CRX-associated congenital blindness. J Clin Invest 2014; 124:631-43. [PMID: 24382353].

18. Bernardo-Colón A, Dong L, Abu-Asab M, Brush RS, Agbaga MP, Becerra SP. Ablation of pigment epithelium-derived factor receptor (PEDF-R/Pnpla2) causes photoreceptor degeneration. J Lipid Res 2023; 64:100358[PMID: 36934843].

19. Doll JA, Stellmach VM, Bouck NP, Bergh AR, Lee C, Abramson LP, Cornwell ML, Pins MR, Borensztajn J, Crawford SE. Pigment epithelium-derived factor regulates the vasculature and mass of the prostate and pancreas. Nat Med 2003; 9:774-80. [PMID: 12740569].

20. Belhadj S, Tolone A, Christensen G, Das S, Chen Y, Paquet-Durand F. Long-Term, Serum-Free Cultivation of Organotypic Mouse Retina Explants with Intact Retinal Pigment Epithelium. J Vis Exp 2020; •••:165-[PMID: 33311434].

21. Romijn HJ. Development and advantages of serum-free, chemically defined nutrient media for culturing of nerve tissue. Biol Cell 1988; 63:263-8. [PMID: 3066424].

22. Bullock J, Polato F, Lulli DC, Sagar V, Abaandou L, Shiloach J, Becerra SP. Expression and production of pigment epithelium-derived factor (PEDF) and PEDF receptor variants from mammalian and bacterial cells. Protein Expr Purif 2022; 194:106072[PMID: 35181508].

23. Zhang X, Feng Q, Cote RH. Efficacy and selectivity of phosphodiesterase-targeted drugs in inhibiting photoreceptor phosphodiesterase (PDE6) in retinal photoreceptors. Invest Ophthalmol Vis Sci 2005; 46:3060-6. [PMID: 16123402].

24. Rebustini IT, Crawford SE, Becerra SP. PEDF Deletion Induces Senescence and Defects in Phagocytosis in the RPE. Int J Mol Sci 2022; 23:7745-[PMID: 35887093].

25. Peng GH, Chen S. Crx activates opsin transcription by recruiting HAT-containing co-activators and promoting histone acetylation. Hum Mol Genet 2007; 16:2433-52. [PMID: 17656371].

26. Chen S, Wang QL, Nie Z, Sun H, Lennon G, Copeland NG, Gilbert DJ, Jenkins NA, Zack DJ. Crx, a novel Otx-like paired-homeodomain protein, binds to and transactivates photoreceptor cell-specific genes. Neuron 1997; 19:1017-30. [PMID: 9390516].

27. Ruzycki PA, Zhang X, Chen S. CRX directs photoreceptor differentiation by accelerating chromatin remodeling at specific target sites. Epigenetics Chromatin 2018; 11:42-[PMID: 30068366].

28. Peng GH, Ahmad O, Ahmad F, Liu J, Chen S. The photoreceptor-specific nuclear receptor Nr2e3 interacts with Crx and exerts opposing effects on the transcription of rod versus cone genes. Hum Mol Genet 2005; 14:747-64. [PMID: 15689355].

29. Comitato A, Schiroli D, La Marca C, Marigo V. Differential Contribution of Calcium-Activated Proteases and ER-Stress in Three Mouse Models of Retinitis Pigmentosa Expressing P23H Mutant RHO. Adv Exp Med Biol 2019; 1185:311-6. [PMID: 31884630].

30. Han J, Dinculescu A, Dai X, Du W, Smith WC, Pang J. Review: the history and role of naturally occurring mouse models with Pde6b mutations. Mol Vis 2013; 19:2579-89. [PMID: 24367157].

31. Berridge MJ, Lipp P, Bootman MD. The versatility and universality of calcium signalling. Nat Rev Mol Cell Biol 2000; 1:11-21. [PMID: 11413485].

32. Mozolewski P, Jeziorek M, Schuster CM, Bading H, Frost B, Dobrowolski R. The role of nuclear Ca2+ in maintaining neuronal homeostasis and brain health. J Cell Sci 2021; 134:jcs254904[PMID: 33912918].

33. Turunen T, Koskelainen A. Functional modulation of phosphodiesterase-6 by calcium in mouse rod photoreceptors. Sci Rep 2021; 11:8938-[PMID: 33903621].

34. Anguissola S, McCormack WJ, Morrin MA, Higgins WJ, Fox DM, Worrall DM. Pigment epithelium-derived factor (PEDF) interacts with transportin SR2, and active nuclear import is facilitated by a novel nuclear localization motif. PLoS One 2011; 6:e26234[PMID: 22028839].

35. Aymerich MS, Alberdi EM, Martínez A, Becerra SP. Evidence for pigment epithelium-derived factor receptors in the neural retina. Invest Ophthalmol Vis Sci 2001; 42:3287-93. [PMID: 11726635].

36. Mottillo EP, Zhang H, Yang A, Zhou L, Granneman JG. Genetically-encoded sensors to detect fatty acid production and trafficking. Mol Metab 2019; 29:55-64. [PMID: 31668392].

37. Palikaras K, Tavernarakis N. Nuclear lipid droplets: a novel regulator of nuclear homeostasis and ageing. Aging (Albany NY) 2024; 16:13436-41. [PMID: 39656091].

38. Ledeen RW, Wu G. Nuclear lipids: key signaling effectors in the nervous system and other tissues. J Lipid Res 2004; 45:1-8. [PMID: 14595003].

39. Hu HT, Wang UT, Chen BC, Hsueh YP, Wang TF. Ki-67 and CDK1 control the dynamic association of nuclear lipids with mitotic chromosomes. J Lipid Res 2025; 66:100731[PMID: 39706365].

40. Cascianelli G, Villani M, Tosti M, Marini F, Bartoccini E, Magni MV, Albi E. Lipid microdomains in cell nucleus. Mol Biol Cell 2008; 19:5289-95. [PMID: 18923143].

41. Bibb LC, Holt JK, Tarttelin EE, Hodges MD, Gregory-Evans K, Rutherford A, Lucas RJ, Sowden JC, Gregory-Evans CY. Temporal and spatial expression patterns of the CRX transcription factor and its downstream targets. Critical differences during human and mouse eye development. Hum Mol Genet 2001; 10:1571-9. [PMID: 11468275].

Articles are provided courtesy of Emory University and The Abraham J. & Phyllis Katz Foundation. The print version of this article was created on 25 September 2026. This reflects all typographical corrections and errata to the article through that date. Details of any changes may be found in the online version of the article.